Journal of
Nanoscience and Nanotechnology
Vol. 10, 6840–6844, 2010

# Electrical Scanning Probe Microscopy of an Integrated Blocking Layer

Stefan A. L. Weber[1,*], Mine Memesa[1], Rüdiger Berger[1], Hans-Jürgen Butt[1], and Jochen S. Gutmann[1,2]

[1] *Max Planck Institute for Polymer Research, Ackermannweg 10, 55128 Mainz, Germany*
[2] *Institute of Physical Chemistry, University Mainz, 55099 Mainz, Germany*

Scanning probe microscopy was performed on an integrated blocking layer system developed for hybrid organic solar cells. A nanocomposite consisting of titania and an amphiphilic triblock copolymer ((PEO)MA-PDMS-MA(PEO)) was prepared by sol–gel chemistry. After plasma treatment and annealing of a spin casted film of 30–100 nm thickness a granular structure with a typical titania grain diameter of 20 nm was found. Conductive scanning force microscopy revealed that on top of almost every grain on the surface there is an increased conductivity compared to the average value. The correlation of grains and conductivity indicated that titania particles formed interconnecting paths through the film. For the resistivity of these pathways we found that effects of tip-sample and sample-electrode resistivity dominate. Additionally, conductive scanning force microscopy revealed non-conducting structures attributed to the thermal treatment. Kelvin probe microscopy of pristine samples on one side and plasma treated plus annealed samples on the other side showed that there is a shift in work function ($0.8 \pm 0.2$ eV) as expected for the transition of amorphous to anatase titania.

**Keywords:** Blocking Layer, Hybrid Solar Cell, Conductive Scanning Force Microscopy, Scanning Kelvin Probe Microscopy.

## 1. INTRODUCTION

Morphology and electrical properties on a nanometer scale play an important role for the development of organic and hybrid solar cells. Typical charge carrier mobilities, exciton binding energies and optical absorption coefficients require a large interfacial area between the donor and acceptor material.[1] These so called bulk heterojunctions have a typical structure size of some nm up to 100 nm. Scanning Force Microscopy (SFM) methods can image the topography of samples at a nanometer resolution. Simultaneously, various additional surface properties can be recorded, e.g., surface charge, tip-sample currents, or workfunction.[2,3] Local electrical currents through samples can be mapped by Conductive Scanning Force Microscopy (CSFM). During contact mode imaging a bias voltage is applied between a metal coated tip and a sample while the local current is mapped (Fig. 1(a)). This technique has recently been used for the characterization of organic solar cell materials. Conductivity maps were obtained on a nanometer scale and at defined positions current–voltage characteristics were recorded.[4–8] In addition, optoelectronic devices are made from material composites having well matched work functions. Thus the work function of surfaces is a material characteristic that needs to be considered on a local scale as well. The scanning force microscope can be operated as a Scanning Kelvin Probe Microscope (SKPM) allowing to determine the work function of a surface with an accuracy of 10 mV at a lateral resolution of 10–20 nm (Fig. 1(b)).[9] With the SKPM and CSFM methods the structure and charge carrier generation mechanisms of organic solar cells have been studied on the nanometer scale.[9,10]

In hybrid organic solar cells an electrically insulating blocking layer between the electrode and the nanoporous inorganic electron acceptor material is essential to prevent short-circuiting and current loss through recombination at the electrode interface. Much effort has been invested into the development of suitable blocking layers.[11] Recently, we developed an integrated blocking layer in a nanocomposite of conducting titania nanoparticles embedded in an insulating polymer derived ceramic matrix.[12,13] Here we report on the local electrical properties on this hybrid layer. With CSFM we studied the effect of different titania contents, whereas the effects of the preparation procedure were investigated by SKPM.

*Author to whom correspondence should be addressed.


1533-4880/2010/10/6840/005 doi:10.1166/jnn.2010.2974

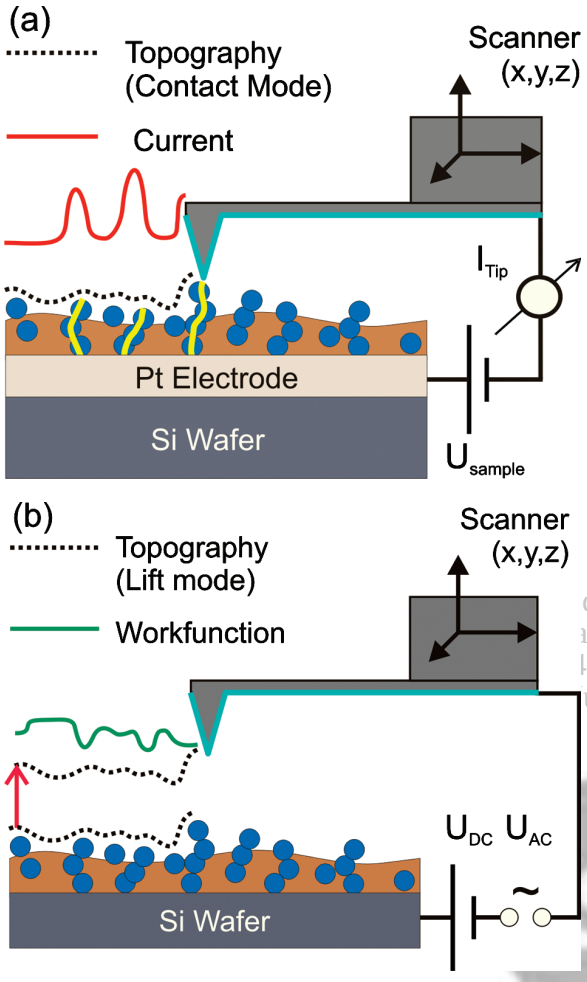


**Fig. 1.** Measurement principles of (a) Conductive Scanning Force Microscopy (CSFM) and (b) Scanning Kelvin Probe Microscopy (SKPM). In CSFM the local conductivity is mapped during Contact Mode Imaging, whereas in KPM the local workfunction is measured in an interleaved step between two topography lines, where the tip is lifted at a certain height.

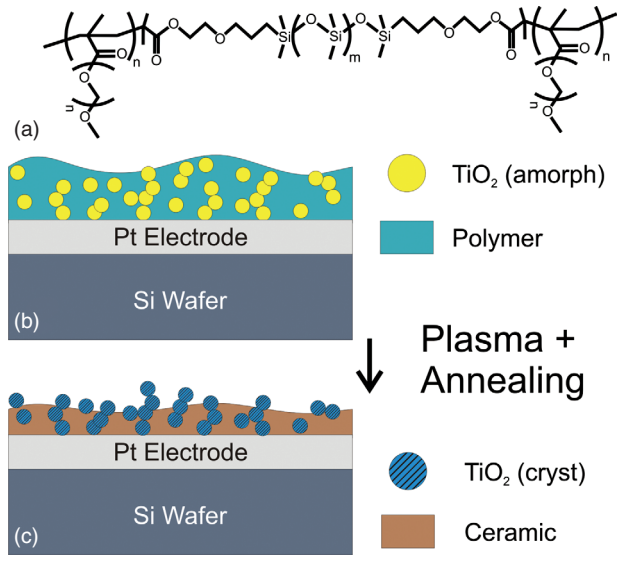


**Fig. 2.** (a) Structure of the (PEO)MA-PDMS-MA(PEO) triblock copolymer.[10] (b) and (c) Schematic of the Sample Preparation. After spin-casting of the titania precursor/triblock copolymer mixture (b) the sample is plasma treated and annealed at 450 °C, leaving a percolated titania network embedded in an electrically insulating matrix of ceramized silicon oxycarbide (c).

## 2. EXPERIMENTAL DETAILS

### 2.1. Sample Preparation

The nanocomposite samples with the hybrid blocking layer were prepared by poly(ethyleneglycol)methylether-methacrylate- block- poly (dimethylsiloxane)- block- poly (ethyleneglycol) methylethermethacrylate ((PEO)MA-PDMS-MA(PEO)) as shown in Figure 2(a).[12] The titania/triblock copolymer nanocomposite was prepared by Sol/Gel chemistry together with titanium tetraisopropoxide (TTIP). Samples with 2% and 5% TTIP content in the stock solution (called for simplicity 2-TTIP and 5-TTIP) and a reference sample with pure polymer were spun cast on a 50 nm thick sputtered Pt-electrode on a silicon wafer (Fig. 2(b)). The Pt-layer acted as counterelectrode for CSFM (Fig. 1(a)). For the SKPM experiments, a second set of samples was prepared in the same way at a TTIP content of 2% directly on a highly doped Silicon substrate (SiMat, CZ, N/Sb, resistivity 0.01–0.02 Ωcm, Fig. 1(b)). Then all samples were treated in Argon plasma at a power of 300 W for 10 min in order to etch away the polymer from the top parts of the sample. Afterwards samples were annealed at 450 °C in $N_2$ atmosphere. During the annealing step, the amorphous titania aggregates transform to anatase $TiO_2$,[12] whereas the PDMS part of the copolymer ceramizes into an insulating silicon oxycarbide matrix (Fig. 2(c)). The film thickness was measured with a surface profiler (Tencor P-10). The 5-TTIP sample was found to be approximately three times thicker ($102 \pm 7$ nm) than the film of the 2-TTIP sample ($30 \pm 6$ nm).

### 2.2. Scanning Probe Microscopy

For CSFM (Multimode SFM extended with a TUNA current amplifier, sensitivity: 1 pA/V, Veeco, Santa Barabara, USA) Pt/Ir coated SPM tips (nominal resonance frequency of 70 kHz, tip radii of curvature 10–20 nm, Nanosensors PPP-EFM) were used. The experiments were performed at a sample bias voltage of 2–3 V on the plasma treated and annealed samples.

The surface workfunction was measured by Scanning Kelvin Probe Microscopy (SKPM; Veeco Dimension 3100 System; Si Cantilevers from Olympus (OMCL-AC240TS, Japan), nominal resonance frequency of 70 kHz.). Here, the tip follows the topography at a defined lift height in an interleaved step between two scan cycles. The lift height was adjusted as low as possible (typically 10 to 20 nm below the average tip height during non contact imaging;

see also Fig. 1(b)); allowing the highest lateral resolution. A certain influence of the scan height on the measured surface potential has been reported.[14] However we observed only a small influence of the scan height on the measured signals, which was below the error margin of our work function results.

## 3. RESULTS AND DISCUSSION

The topography of 2-TTIP and 5-TTIP samples showed a similar granular structure with a typical grain diameter of 20 nm and a root-mean-square (RMS) roughness of 0.5 nm (Figs. 3(Ia and IIa)). The grain structure is attributed to the titania particles. Thus, we conclude that the average diameter and the number of titania particles at the surface in both films are similar.

The current maps revealed that on both samples almost every grain on the surface was associated with a current which was well above the current map mean value of 0.3 pA (Figs. 3(Ib and IIb)). The correlation of grains and currents proved that the conductivity was caused by the titania particles which formed an interconnection to the Pt-electrode, whereas the gaps between the particles were electrically insulating. We found that the correlation of topography and conductivity in the 2-TTIP and 5-TTIP sample were similar. The increased film thickness of 5-TTIP ($102 \pm 7$ nm) compared to the 2-TTIP sample ($30 \pm 6$ nm) results in an increase in the number of titania particles in one percolation path. However, the interconnection between adjacent titania particles remain similar. Thus the conductivity should decrease with increasing film thickness. We observed that the distribution of the conductance $I/U_{\text{Sample}}$ over both samples revealed a very similar behavior (Fig. 4). Therefore the determined $I/U_{\text{Sample}}$ is not limited by the resistivity of the titania network, but rather by the contact resistance at the platinum-titania and the titania-tip interface.

Furthermore, in both samples insulating areas, 100 nm in width, were observed. Most of these areas could be associated with elevations in the topography, 2–6 nm in height (e.g., the two adjacent spots in Figs. 3Ia and one in IIa, yellow arrows). Scanning larger areas showed that these insulating spots occurred at a density of 2–3 per $\mu m^2$. These structures might be caused by the annealing of the samples which leads to thermal stress. At defect sites the film buckles and upon cooling the brittle film can collapse. This interpretation is supported by the finding that in the center of larger elevations, small depressions 10–15 nm in diameter and 5 nm in depth occurred.

In order to show that the conductivity measured in the previous experiments is solely caused by the titania particles, a pure polymer film on platinum after annealing was studied for reference. This film had a thickness of $(77 \pm 1)$ nm and no conductance could be found at a bias voltage of 3 V at the highest current sensitivity.

Complementary SKPM was performed to further elucidate material changes induced by annealing. For these measurements we compared pristine with plasma treated/annealed 2-TTIP samples. In contrast to CSFM, SKPM can be operated in a non-contact mode allowing non-destructive imaging of soft surfaces which is the case for the pristine sample. During the interleaved step, the contact potential difference $V^{\text{CPD}}$ (i.e., the difference in workfunction $\Delta\Phi = eV^{\text{CPD}}$, $e$: elemental charge) of the SFM-tip and sample surface was measured.[15] In order to determine the absolute value $\Phi_{\text{Sample}}$ of the work function of the investigated sample surfaces, reference



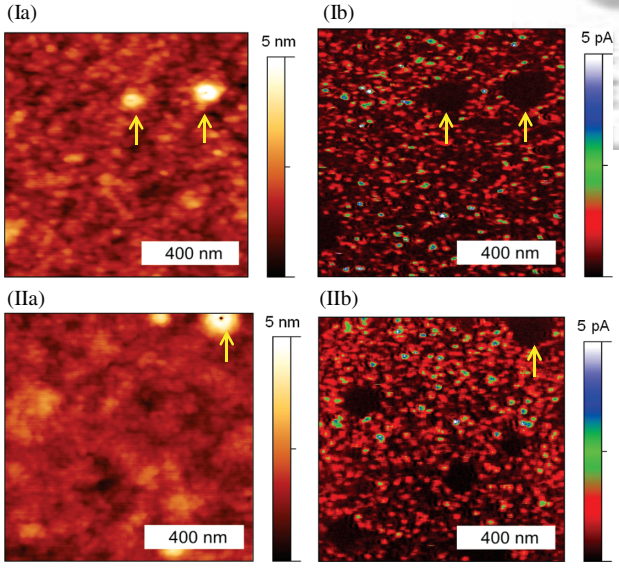


**Fig. 3.** Topography (Ia, IIa) and current map (Ib, IIb) of the plasma treated and annealed 2-TTIP (Ia, b) and 5-TTIP (IIa, b) sample obtained with CSFM. Localized conduction paths with currents up to 7 pA can be observed in both samples. Furthermore, insulating patches were observed, which can be associated with ~100 nm wide and 2–5 nm high elevations (yellow arrows).

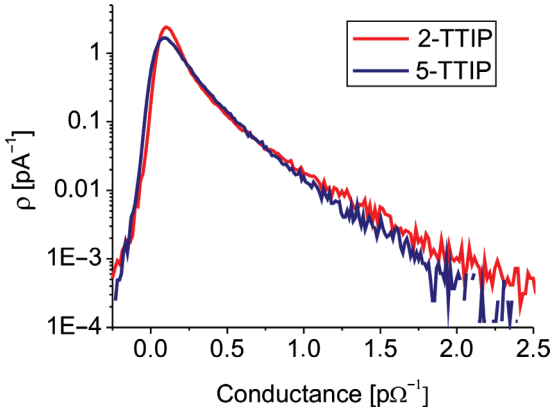


**Fig. 4.** Electrical conductance ($I/U_{\text{Sample}}$) distribution on the 2-TTIP samples (red line) and 5-TTIP sample (blue line). Only small deviations from the exponential decay towards higher conductance values were found. A slightly higher conductance and stronger deviations can be seen on the 2-TTIP sample. Negative values are due to noise and overshoots caused by the electronics.

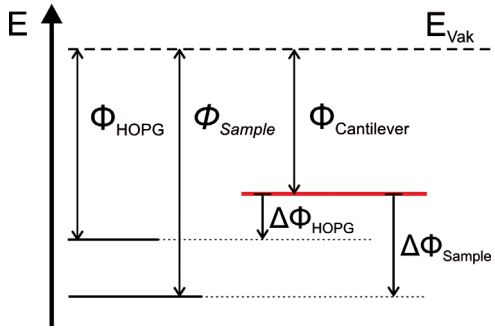


**Fig. 5.** Schematic representation of the relevant energy levels for KPM. During the measurement, the contact potential difference, $\Delta\Phi_{Sample}$, of SFM-tip (red line) and sample surface is measured. By comparing this value with a reference sample ($\Phi_{HOPG}$) the unknown $\Phi_{Sample}$ is determined.

measurements on freshly cleaved HOPG substrates having a known workfunction of $\Phi_{HOPG} = 4.5$ eV[16] were performed for each SFM tip. With the sample signal $V^{CPD}_{sample}$ and the reference signal $V^{CPD}_{HOPG}$ the absolute value can be calculated by[16] (Fig. 5)

$$\Phi_{Sample} = \Phi_{HOPG} + e(V^{CPD}_{sample} - V^{CPD}_{HOPG})$$

From SPM we found that the topography of pristine and annealed 2-TTIP sample showed no differences (Figs. 6(Ia and IIa)). In SPM, a material contrast can be obtained by recording the phase contrast.[17] In our case the phase contrast did not reveal a significant difference (Figs. 6(Ib and IIb)). This observation indicates that the particles were closely packed and that the amount of polymer which is situated between the particles is not sufficient to cause a measurable material contrast in the pristine sample. However the plasma treatment and annealing step resulted in

(i) a removal of polymer from surfaces,
(ii) the ceramization of the PDMS and
(iii) a transition to anatase titania particles (Figs. 2(b to c)).

Thus, the surface potential is supposed to change. SKPM experiments revealed a clear shift in work function from $(3.7 \pm 0.1)$ eV to $(4.5 \pm 0.1)$ eV, from the pristine to the plasma treated and annealed sample surface (Figs. 6(Ic and IIc)). In all pristine samples, we observed that the work function changed during scanning, i.e., from top to bottom in the shown example of Figure 6(Ic). This decrease in work function can be attributed to the gradual contamination of the SFM-tip by the soft (PEO)MA-PDMS-MA(PEO) during scanning.[15] Such a pronounced decrease in surface potential was not observed on the plasma treated and annealed samples, which additionally indicated the conversion of the soft (PEO)MA-PDMS-MA(PEO) at the sample surface into a hard inorganic material.



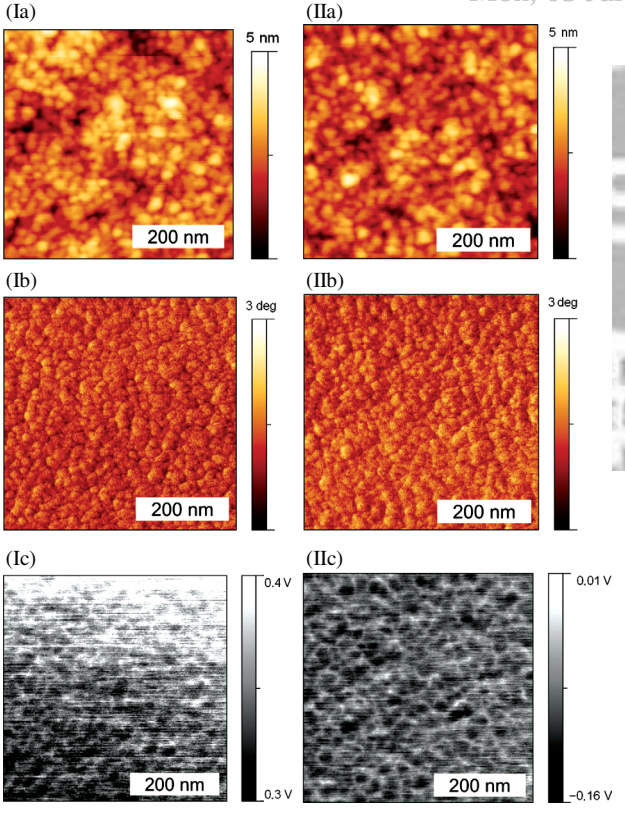


**Fig. 6.** KPM study of pristine (I) and plasma treated and annealed (II) titania/(PEO)MA-PDMS-MA(PEO) nanocomposite films: (a) topography, (b) phase, (c) potential. No significant changes in the topography and phase can be observed ((Ia): roughness on $(500\ nm)^2$ RMS = 0.6 nm, IIa: roughness on $(500\ nm)^2$ RMS = 0.6 nm). However, the absolute work function was shifted from $(3.7 \pm 0.1)$ eV for the as prepared sample (Ic) to $(4.5 \pm 0.1)$ eV for the plasma treated and annealed sample (IIc) (Note: The scale bars in Ic and IIc represent the contact potential difference between tip and sample; see text for further explanation).

## 4. SUMMARY

Conductive probe microscopy and Kelvin probe microscopy measurements showed that the concept of an integrated barrier layer in a nanopourous titania network derived from (PEO)MA-PDMS-MA(PEO) triblock copolymer[12] is feasible. The experiments proved the existence of isolated conductive percolation paths composed of titania particles embedded in an insulating matrix. The statistical analysis of the conductance showed an exponential decay towards higher current values that has been calculated for random resistor networks.[18] However in the present system, tip-sample and sample-electrode resistivity dominate in the measured current values and must be considered.

**Acknowledgment:** The financial support from the Max Planck Society, the Korean-German IRTG "Self organized materials for Optoelectronics" (DFG Graduiertenkolleg 1404) and the German Science Foundation (SPP 1181, GU771/2 and MU1487/5) is gratefully acknowledged.

## References and Notes


1. H. Hoppe and N. S. Sariciftci, Advances in Polymer Science, Photoresponsive Polymers II, Springer Berlin/Heidelberg **(2008)**, Vol. 214, p. 1.
2. R. Berger, H.-J. Butt, M. B. Retschke, and S. A. L. Weber, *Macromol. Rapid Commun.* 30, 1167 **(2009)**.
3. L. S. C. Pingree, O. G.. Reid, and D. S. Ginger, *Adv. Mat.* 21, 19 **(2009)**.
4. O. Douhéret, A. Swinnen, S. Bertho, I. Haeldermans, J. D'Haen, M. D'Olieslaeger, D. Vanderzande, and J. V. Manca, *Progress in Photovoltaics: Research and Applications* 15, 713 **(2007)**.
5. A. Alexeev, J. Loos, and M. M. Koetse, *Ultramicroscopy* 106, 191 **(2006)**.
6. O. Douhéret, L. Lutsen, A. Swinnen, M. Breselge, K. Vandewal, L. Goris, and J. Manca, *Appl. Phys. Lett.* 89, 032107 **(2006)**.
7. D. C. Coffey, O. G. Reid, D. B. Rodovsky, G. P. Bartholomew, and D. S. Ginger, *Nano Lett.* 7, 738 **(2007)**.
8. M. Dante, J. Peet, and T.-Q. Nguyen, *J. Phys. Chem. C* 112, 7241 **(2008)**.
9. V. Palermo, M. Palma, and P. Samorì, *Adv. Mater.* 18, 145 **(2006)**.
10. H. Hoppe, T. Glatzel, M. Niggemann, A. Hinsch, M. Ch. Lux-Steiner, and N. S. Sariciftci, *Nano Lett.* 5, 269, **(2005)**.
11. B. Peng, G. Jungmann, C. Jäger, D. Haarer, H. W. Schmidt, and M. Thelakkat, *Coordin. Chem. Rev.* 248, 1479 **(2004)**.
12. M. Memesa, S. Weber, S. Lenz, J. Perlich, R. Berger, P. Müller-Buschbaum, and J. S. Gutmann, *Energy & Environ. Sci.* 2, 783 **(2008)**.
13. Y. J. Cheng and J. S. Gutmann, *J. Am. Chem. Soc.* 128, 4658 **(2006)**.
14. A. Liscio, V. Palermo, K. Müllen, and P. Samori, *J. Phys. Chem. C* 112, 17368 **(2008)**.
15. H. O. Jacobs, H. F. Knapp, and A. Stemmer, *Rev. Sci. Instrum.* 70, 1756 **(1999)**.
16. W. N. Hansen and G. J. Hansen, *Surf. Sci.* 481, 172 **(2001)**.
17. S. N. Magonov and N. A. Yerina, *Langmuir* 19, 500 **(2003)**.
18. G. G. Batrouni, A. Hansen, and B. Larson, *Phys. Rev. E* 53, 2292 **(1996)**.


Received: 1 November 2008. Accepted: 9 February 2009.